

Modelling deep convection and its impacts on the tropical tropopause layer

J. S. Hosking^{1,*}, M. R. Russo², P. Braesicke², and J. A. Pyle²

¹Centre for Atmospheric Science, University of Cambridge, Cambridge, UK

²NCAS, University of Cambridge, Cambridge, UK

*now at: the British Antarctic Survey, Cambridge, UK

Received: 22 July 2010 – Published in Atmos. Chem. Phys. Discuss.: 26 August 2010

Revised: 18 November 2010 – Accepted: 22 November 2010 – Published: 26 November 2010

Abstract. The UK Met Office's Unified Model is used at a climate resolution (N216, $\sim 0.83^\circ \times \sim 0.56^\circ$, ~ 60 km) to assess the impact of deep tropical convection on the structure of the tropical tropopause layer (TTL). We focus on the potential for rapid transport of short-lived ozone depleting species to the stratosphere by rapid convective uplift. The modelled horizontal structure of organised convection is shown to match closely with signatures found in the OLR satellite data. In the model, deep convective elevators rapidly lift air from 4–5 km up to 12–14 km. The influx of tropospheric air entering the TTL (11–12 km) is similar for all tropical regions with most convection stopping below ~ 14 km. The tropical tropopause is coldest and driest between November and February, coinciding with the greatest upwelling over the tropical warm pool. As this deep convection is co-located with bromine-rich biogenic coastal emissions, this period and location could potentially be the preferential gateway for stratospheric bromine.

in which many quantities undergo a gradual transition from their tropospheric to their stratospheric characteristics. This Tropical Tropopause Layer (TTL) can be defined in many ways (see review by Fueglistaler et al., 2009), including thermally as a region between a lapse rate minimum (LRM) and the tropical tropopause (Highwood and Hoskins, 1998; Gettelman and Forster, 2002). Within the tropics, between these upper and lower TTL boundaries also lies the clear-sky level of zero radiative heating ($Q_{\text{clear}} = 0$). The $Q_{\text{clear}} = 0$ level separates the broad regions of radiative ascent (above) and subsidence (below). For the purpose of this paper we define the “lower TTL” as the region between the lapse-rate minimum (LRM) and the $Q_{\text{clear}} = 0$ level, and the “upper TTL” as the region between the $Q_{\text{clear}} = 0$ level and the tropopause.

The permeability of this region for fast transport from the troposphere to the stratosphere depends crucially on its interplay with convection (Seidel et al., 2001; Gettelman and Forster, 2002). Fast transport of boundary layer air, potentially rich in very short lived (halogenated) species (VSLS) of maritime origin, into the stratosphere could help to explain elevated observations of stratospheric inorganic bromine (Br_y) of between 18 and 25 ppt (Salawitch et al., 2005). Note that brominated VSLS such as bromoform (CHBr_3) are generally ignored within stratospheric chemistry-climate models. Their relatively short lifetimes (26 days and less) and slow radiatively driven ascent rates around the tropical tropopause seemed to indicate only a minor role in stratospheric chemistry. Nevertheless, this simplification might be one reason why current atmospheric models underestimate the amount of bromine present in the stratosphere by about 20% (Salawitch et al., 2005) and subsequently the potential for ozone loss.

The permeability of the TTL is determined by two mechanisms; (1) by a direct, convectively driven, air mass injection into the TTL followed by slower radiative ascent during which air moves quasi-horizontally and passes through the tropopause (Sherwood and Dessler, 2000); or (2) by

1 Introduction

The tropics have long been recognized as a primary gateway for tropospheric air entering the stratosphere (Brewer, 1949). The exact nature of how air crosses the tropical tropopause is key to determining the water vapour content and chemical boundary conditions of the stratosphere (Holton and Gettelman, 2001; Sinnhuber and Folkins, 2006). The notion of the tropical tropopause as a sharp discontinuity simultaneously present in many quantities, like temperature, water vapour and ozone, has been dropped in recent years (Folkins et al., 1999). Instead it has become increasingly evident that the tropical tropopause is best described as a transition layer,



Correspondence to: J. S. Hosking
(scott.hosking@atm.ch.cam.ac.uk)

an irreversible direct convective air mass injection into the stratospheric overworld (Danielsen, 1993). Both mechanisms require a detailed understanding of how convection interacts with the TTL. Note that (1) does not exclude fast “sideways” transport into the extra-tropical lowermost stratosphere (e.g., Levine et al., 2007), and that many trajectory studies are able to reproduce water vapour distributions in the lowermost stratosphere successfully based on this mechanism. Observational evidence for (2) seems inconclusive. Gettelman et al. (2002), Liu and Zipser (2005), and Rossow and Pearl (2007) using satellite data found that only 0.5–1 percent of storms penetrate the stratosphere. However, Ricaud et al. (2007) observed clear and persistent trace gas anomalies, including N_2O , CH_4 and CO , at heights around 16–17 km, just above the tropopause. This also agrees with the presence of ice particles at 420 K observed during the EU FP7 project SCOUT-O3 (Corti et al., 2008). Therefore, although direct convective injections into the lower stratosphere have been observed, their frequency and relative impact on stratospheric composition is still debated.

Vertically the release of latent heat below 14 km is an important factor in establishing the environmental lapse rate of the tropospheric temperature profile. Consequently the direct impact of tropospheric convection on the thermal structure of the upper TTL is small compared to the free troposphere. Horizontally the longitudinally varying TTL structure is difficult to assess from observations and in models, because convection varies significantly from region to region and has many different temporal characteristics, including diurnal and seasonal cycles. This enforces the notion that mechanism (2) is not easily detectable, but may have regional importance. It is conceivable that in some areas particularly strong convection events might be able to penetrate through the upper TTL into the stratosphere (Sassen et al., 2008; Nazaryan et al., 2008).

To disentangle the two mechanisms and to provide insights into how a state-of-the-art atmospheric model represents the TTL and its interaction with convection, we use a weather forecasting model. The model used is the Met Office’s Unified Model (UM) with an approximate resolution of 60 km ($\text{N}216$, $\sim 0.83^\circ \times \sim 0.56^\circ$). The overarching aims of this paper are to determine:

1. How well does the model represent the mean location of deep tropical convection?
2. Is fast tropical convective transport in the model significant and does this mechanism potentially affect the composition and structure of the TTL?

Recent studies provide further evidence that this very model setup is suitable for transporting VLSLs as shown by comparing the distribution of modelled high cloud to observations (Russo et al., 2010) and vertical convective transport of idealised short-lived tracers (Hoyle et al., 2010).

This analysis allows for the comparison between competing hypotheses for troposphere-stratosphere transport (TST), namely of Newell and Gould-Stewart (1981) who proposed a “Stratospheric Fountain” where the Maritime Continent and West Pacific are the main region for TST, and Liu and Zipser (2005) who argue for many “Stratospheric Fountains” (driven by convection over Africa, Maritime Continent and South America). We also investigate the frequency of deep convection reaching the upper TTL in our model to assess whether stratospheric air mass injection is common (Danielsen, 1993) or uncommon (Highwood and Hoskins, 1998).

Capturing the location of convection is also important for transporting VLSLs (e.g., from coastal regions) as it is likely that convection is the only mechanism by which these species may reach the TTL in significant quantities. Once in the upper TTL, with the increase in residence time (Fueglistaler et al., 2004), radiative ascent and quasi-horizontal transport can drive these VLSLs, and their degradation products, into the lower stratosphere.

In confronting the model’s performance against observational evidence we develop confidence in the reliability of our model results. Monthly mean OLR and precipitation rate are used to compare the regional distribution of tropical convective activity between the models and satellite. Figure 1 shows regions of low OLR for November 2005 using a 240 Wm^{-2} contour from satellite (Panel a) and the spatial relationship between low OLR and convective activity in the model where convection is measured by two methods: Panel b illustrates the frequency of convective cloud top reaching the upper TTL ($\gtrsim 14.5 \text{ km}$) while Panel c shows the monthly mean convective mass flux integrated over the lower TTL. From this figure, there are two key questions which we will address: How does the location of OLR match convection in the model? and, How does OLR compare between the model and observations?

The detailed experimental methodology and model setup will be outlined in Sect. 2. In Sect. 3, model simulations will be validated with monthly mean OLR and precipitation satellite observations. Here we assess the ability of a UM forecast model to reproduce the location of convection over the three main tropical convective regions – Africa, the Maritime Continent and South America and describe how their characteristic convective signatures change from one season to the next. The ability of models to represent the TTL structure and convection will be presented within Sect. 4. Finally, Sect. 5 will summarise these findings.

2 Methodology

In this study we use the Met Office Unified Model (UM) version 6.1 (Davies et al., 2005). This model is extensively used both as a weather forecast tool at various National

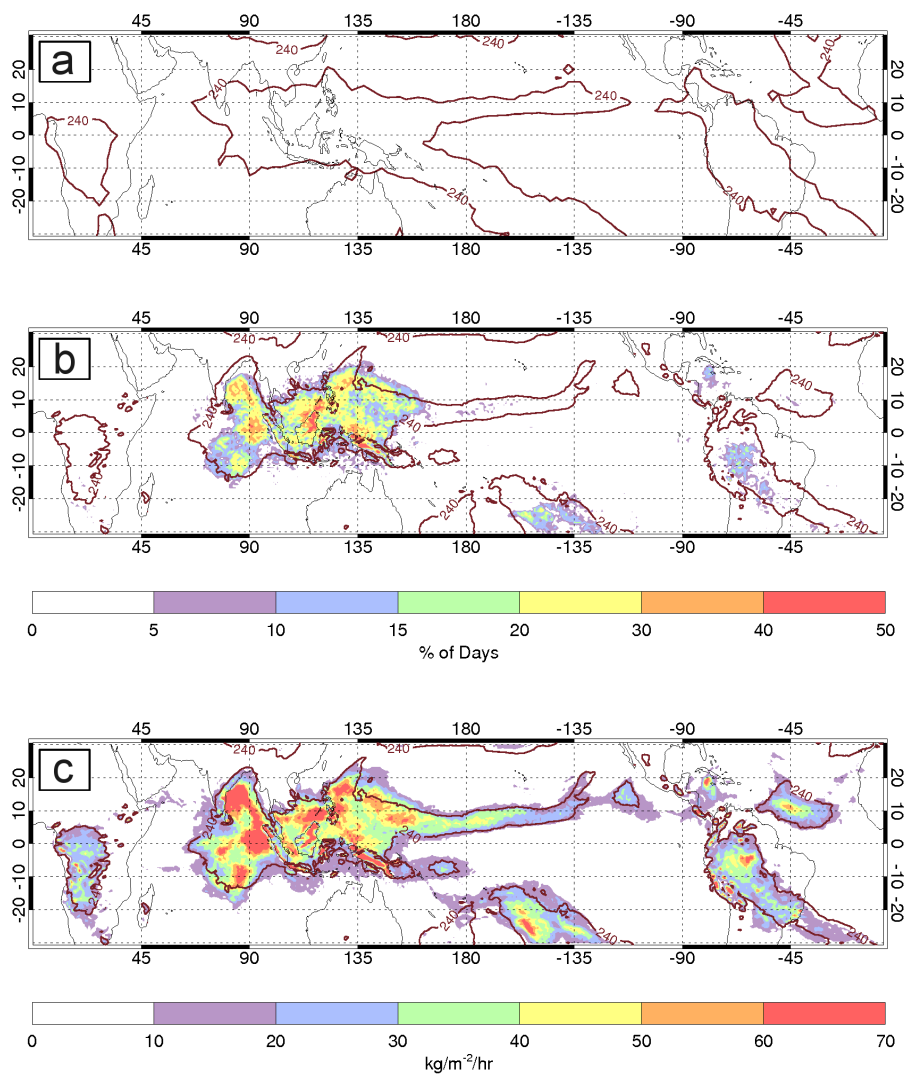


Fig. 1. Monthly mean satellite data (Panel a) is compared to the UM forecast model integration for November 2005 (Panels b and c). The red lines show the OLR 240 Wm^{-2} contour. Shaded contours represent the frequency of convective cloud top reaching the upper TTL (Panel b); and the monthly mean convective mass flux integrated over the lower TTL (Panel c).

Meteorological Centres around the world, and as a climate model in recent Climate Assessment Reports.

The model surface is represented using the MOSES (Met Office Surface Exchange Scheme) surface hydrology and soil model scheme (Essery et al., 2003). The Boundary Layer parametrisation is non-local in unstable regimes (Lock et al., 2000). The convective parametrisation scheme is based on Gregory and Rowntree (1990) and is called by the model twice per timestep where the timestep adopted is 20 min – the default for the UM forecast setup. Both shallow and deep convection are included in the scheme. Cloud base closure for shallow convection is based on Grant (2001), and parametrised entrainment and detrainment rates for shallow convection are obtained from Grant and Brown (1999). For deep convection, the thermodynamic closure is based on

the reduction of the convectively available potential energy, CAPE, to zero (CAPE closure approach) based on Fritsch and Chappell (1980a,b). The CAPE timescale, which determines the e-folding time for the dissipation of CAPE, is set to the tried and tested default value of 30 min (i.e., the cloud based mass flux is relaxed to an equilibrium state over 1.5 timesteps where the convection scheme is called 3 times). A detailed representation of cloud microphysics is achieved using physically based parametrisation for transfers between the different categories of hydrometeors (Wilson and Ballard, 1999). Radiative transfer is calculated using the Edwards-Slingo radiation scheme (Edwards and Slingo, 1996).

We run a weather forecast configuration based on a recent operational weather forecast setup used at the UK Met Office until December 2005 and was used in a recent

GCSS (GEWEX, Global Energy and Water Cycle Experiment, Cloud System Study) comparison study of deep convection over the Tropical West Pacific (Petch et al., 2007). The vertical resolution is composed from a hybrid sigma-height coordinate system with 38 vertical levels and a model top at ~ 40 km, and a horizontal resolution of $\sim 0.83^\circ \times 0.56^\circ$ (N216). The vertical model resolution around the height of the TTL is ~ 1 km (i.e., between 10 and 17 km). In Sect. 4.2 we compare this setup to the widely used climate setup HadGEM1a (Martin et al., 2006). The climate model, which is run at a much lower horizontal resolution (N96, $\sim 1.87^\circ \times 1.25^\circ$) is setup in the same manner as the forecast setup.

We perform four model runs with the forecast model configuration, each for a separate month in 2005, specifically February, May, August and November. The year 2005 has been chosen since it does not show either a strong *El Niño* or *La Niña* signal. Each of the four model runs is initialised using a UK Met Office data-assimilated start dump for the corresponding month, thus providing an accurate representation of the initial state of the atmosphere. The model is then allowed to run continuously for one month, constrained by GISST 2.0 climatological SST and sea ice (Parker et al., 1995), AMIP climatological soil temperature and soil moisture, and climatological ozone (Li and Shine, 1995). Although the predictability for a forecast model drops significantly after 10 days, we are able to assess the ability of the model to capture the statistical characteristics of convection, such as location, strength and seasonal variations.

All monthly mean diagnostics are calculated over all timesteps except where explicitly mentioned in the text below. Monthly mean results from the forecast setup are degraded to $2.5^\circ \times 2.5^\circ$ and compared to monthly mean satellite maps of Outgoing Longwave Radiation (OLR) from NOAA (Liebmann and Smith, 1996) and Precipitation Rate from CMAP (Xie and Arkin, 1997). We perform a quantitative statistical analysis of model and satellite fields by calculating a “point-by-point” correlation coefficient and the coefficient of variation of the root mean square error¹ (CVRMSE). Precipitation and OLR, used in combination, are a good proxy for the location and intensity of tropical convection, particularly when averaged over a month so that only persistent features are kept in the mean.

The TTL properties to be investigated in the different model calculations include the temperature *Lapse Rate Minimum* (LRM) around 10–12 km, the clear-sky level of zero radiative heating ($Q_{\text{clear}} = 0$) around 14–15 km, and the tropopause around 16–17 km.

There are various definitions of the tropopause in the literature (e.g., Sherwood and Dessler, 2001; Thuburn and Craig, 2002; Gettelman and Forster, 2002). Here, the tropopause will primarily be defined using the *Cold Point Tropopause*

¹RMSE is calculated for the domain in Wm^{-2} and is then converted to a percentage of the domain OLR mean (CVRMSE).

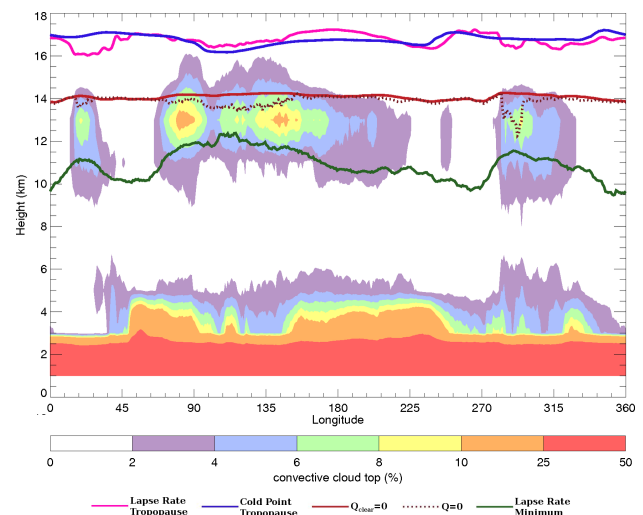


Fig. 2. The longitudinal-vertical distribution of tropical convective cloud tops between latitudes 20° N– 20° S for the modelled November integration. The coloured lines represent surfaces of the tropical tropopause layer as shown by the legend and discussed in Sect. 4.

(CPT) although we will also analyse other commonly used definitions, namely the WMO *Lapse Rate Tropopause* (LRT) and the 380 K isentropic level. These are discussed further in Highwood and Hoskins (1998).

In the model, the LRM, CPT and LRT surfaces are vertically interpolated from monthly mean temperature diagnostics. The level of zero radiative heating is calculated from monthly mean heating rates, either assuming a *cloud free* atmosphere (labelled as $Q_{\text{clear}} = 0$ or “clear-sky”) or allowing condensed water to interact with radiation (labelled $Q = 0$ or “all-sky”). In our model integrations the height of the $Q_{\text{clear}} = 0$ surface is generally similar to or higher than the height of the $Q = 0$ surface, therefore the choice of $Q_{\text{clear}} = 0$ as the lower boundary for the “upper TTL” region ensures that anything reaching the “upper TTL” will be above both “all-sky” and “clear-sky” surfaces.

In Sect. 4.3 we use a novel diagnostic to assess the vertical structure of deep convection by defining a probability density function (PDF) for cloud top heights. The convective cloud cloud top heights are a model diagnostic, derived every 3 h as a longitude-latitude map, indicating the highest altitude to which a cloud penetrated. From this diagnostic we derive at each longitude the number of occurrences of cloud tops in a certain height interval (every 2 km from the surface to 18 km) and within the equatorial belt (20° S– 20° N) over a month. Colour shadings in Fig. 2 show the normalised PDF for November 2005 as a function of longitude and height bin. The normalisation is relative to the number of grid points in the latitudinal belt at a particular longitude multiplied by the number of timesteps in a month and is expressed in percent. A value of for example 10% could indicate that at any time 10% of all latitudinal points indicated a cloud top at this

Table 1. Monthly mean satellite and model OLR spatial correlation coefficients calculated independently for the tropics and the 8 domains between latitudes $\pm 20^\circ$. The modelled data is degraded to the satellite resolution for comparison. Higher values represent a better match between the two sets of data.

Month	Tropics	Africa	India	Maritime C.	W. Pacific	C. Pacific	E. Pacific	S. America	Atlantic
February	0.66	0.81	0.47	0.68	0.66	0.71	0.89	0.88	0.75
May	0.77	0.82	0.72	0.87	0.76	0.57	0.78	0.72	0.50
August	0.83	0.90	0.83	0.90	0.79	0.86	0.94	0.65	0.86
November	0.80	0.87	0.74	0.84	0.79	0.86	0.70	0.74	0.72

Table 2. Monthly mean satellite and model OLR coefficient of variation of the RMSE (CVRMSE) as a percentage calculated independently for the tropics and the 8 domains between latitudes $\pm 20^\circ$. The modelled data is degraded to the satellite resolution for comparison. Lower values represent a better match between the two sets of data.

Month	Tropics	Africa	India	Maritime C.	W. Pacific	C. Pacific	E. Pacific	S. America	Atlantic
February	10.43	9.99	10.07	10.87	11.48	18.07	5.23	8.75	5.59
May	8.22	7.37	8.58	7.17	8.03	9.56	8.28	8.73	7.74
August	8.08	7.35	10.85	7.26	9.24	6.82	6.71	8.59	7.14
November	8.48	6.28	7.79	8.41	10.01	8.39	7.22	10.10	9.43

height, or that 20% of all latitudinal points indicated a cloud top at this height for 50% (half) of the month. This caveat has to be kept in mind when interpreting the PDF figures. In Fig. 2 the cloud top height PDF indicates a probability of around 10–25% in a height region between 12–14 km between the lapse rate minimum and the $Q = 0$ lines. Later, we will discuss the position of such PDF maxima relative to areas of enhanced convective mass flux.

3 Satellite and model comparisons using OLR and precipitation rate

The convective activity diagnostics (Panels b and c in Fig. 1) share the same broad spatial distribution over the Indian Ocean, Maritime Continent and West Pacific where deep convection is frequent. Panel b shows that, for values above 5%², only the Maritime Continent shows a good agreement with the 240 Wm⁻² OLR contours whereas the mass flux diagnostic (Panel c) show that all convective regions display a good fit. The convective mass flux diagnostic highlights that there is also deep convection over Africa, South America and the Intertropical Convergence Zone (ITCZ), lifting material up to the upper TTL. The inconsistency between the spatial patterns of convective activity between the two diagnostics is probably due to the fact that the level of mean convective outflow is somewhere between 12–15 km (Folkens et al., 2000). Therefore, the diagnostic that measures convection over-reaching $Q_{\text{clear}} = 0$ will miss out on any convective

²Values smaller than 5%, 1.5 days in the month, are taken to be insignificant and therefore are not represented by the contour colour scale

cloud tops that are just below this level. Air that detrains from a convective tower in the lower TTL could still be significant for loading trace gases into the upper TTL by another mechanism, e.g., another (later) deep convective event.

Generally, the spatial distribution of low OLR compares well over the tropical convective regions of Africa and the Maritime Continent between the observations and model. The South Pacific Convergence Zone (SPCZ) is less well defined in this model integration. The modelled mass flux contours match the models low OLR signals well for all four months (not shown) illustrating that monthly mean OLR is a proxy for deep and frequent tropical convective activity in the model. A more detailed OLR model-observation comparison for all the monthly integrations used in this paper is presented in Fig. 3.

Even at this relatively high model resolution, the observed deep convective towers (which may only be 1–10 km² in size and last for ~ 10 min) can obviously not be represented by the model. As a result, convectively driven injections directly into the stratosphere are very uncommon in the model. However, the Maritime Continent and West Pacific are far more significant in terms of deep convection compared to Africa and South America which is in agreement with the Newell and Gould-Stewart (1981) “Stratospheric Fountain” hypothesis, and inconsistent with studies made by Liu and Zipser (2005) where analysis of remotely sensed particles with high reflectivity show that the deepest and most frequent convective region is over the Congo basin.

We now analyse the OLR data, as well as precipitation rate, to compare the spatial patterns and intensities between the model and satellite data. In addition, spatial correlation coefficients and CVRMSE are calculated for the monthly

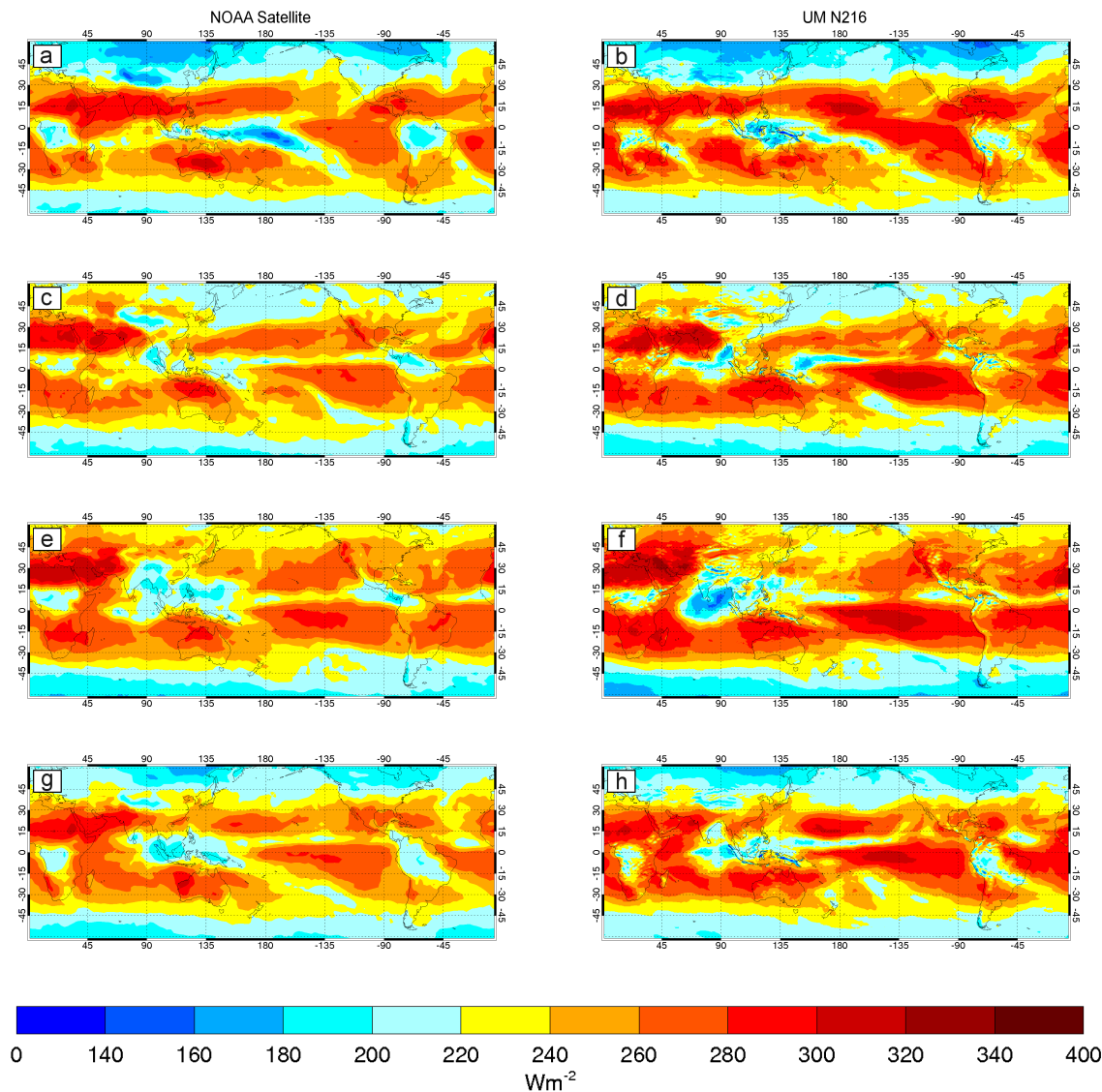


Fig. 3. Monthly mean NOAA OLR satellite data (left column) and UM forecast model experiment (right column) comparisons for February (a, b), May (c, d), August (e, f) and November (g, h) 2005.

mean satellite and model OLR data (Tables 1 and 2, respectively). Here, the tropical belt (20°N – 20°S) is divided into 8 equal regions of 45° in longitude; starting from Africa (0 – 45°E) and finishing with the Atlantic (315 – 360°E). Assuming all points are independent, the correlation coefficients are all significant according to Pearson's one-tailed test at a level of 99.5%.

Figure 3 shows that the large-scale behaviour in the model matches observations, although there are detailed differences in terms of spatial structure and the magnitude of the OLR. For the February integration, the tropical domain correlation coefficient (0.66) and CVRMSE (10.43%) are significantly poorer compared to the May, August and November integrations. This time of year has intense convective activity over

the Maritime Continent and West Pacific (Newell and Gould-Stewart, 1981) as shown, for example, by the very low OLR ($<160\text{Wm}^{-2}$) seen in the satellite OLR at 180°E . However, these intensities are not present in the model suggesting that the convection is underestimated in February. The inconsistency in OLR intensity is also highlighted by the high CVRMSE in the West Pacific box in Table 2.

Figures 3 and 4, for both observations and the model, suggest that the Indian Ocean, Maritime Continent and West Pacific dominate in terms of deep convection. The general variation in OLR is well represented along with the seasonal cycle clearly illustrated in Northern Hemisphere summer (August) where OLR values are higher in both the observations and model. Equatorial Africa, Maritime Continent

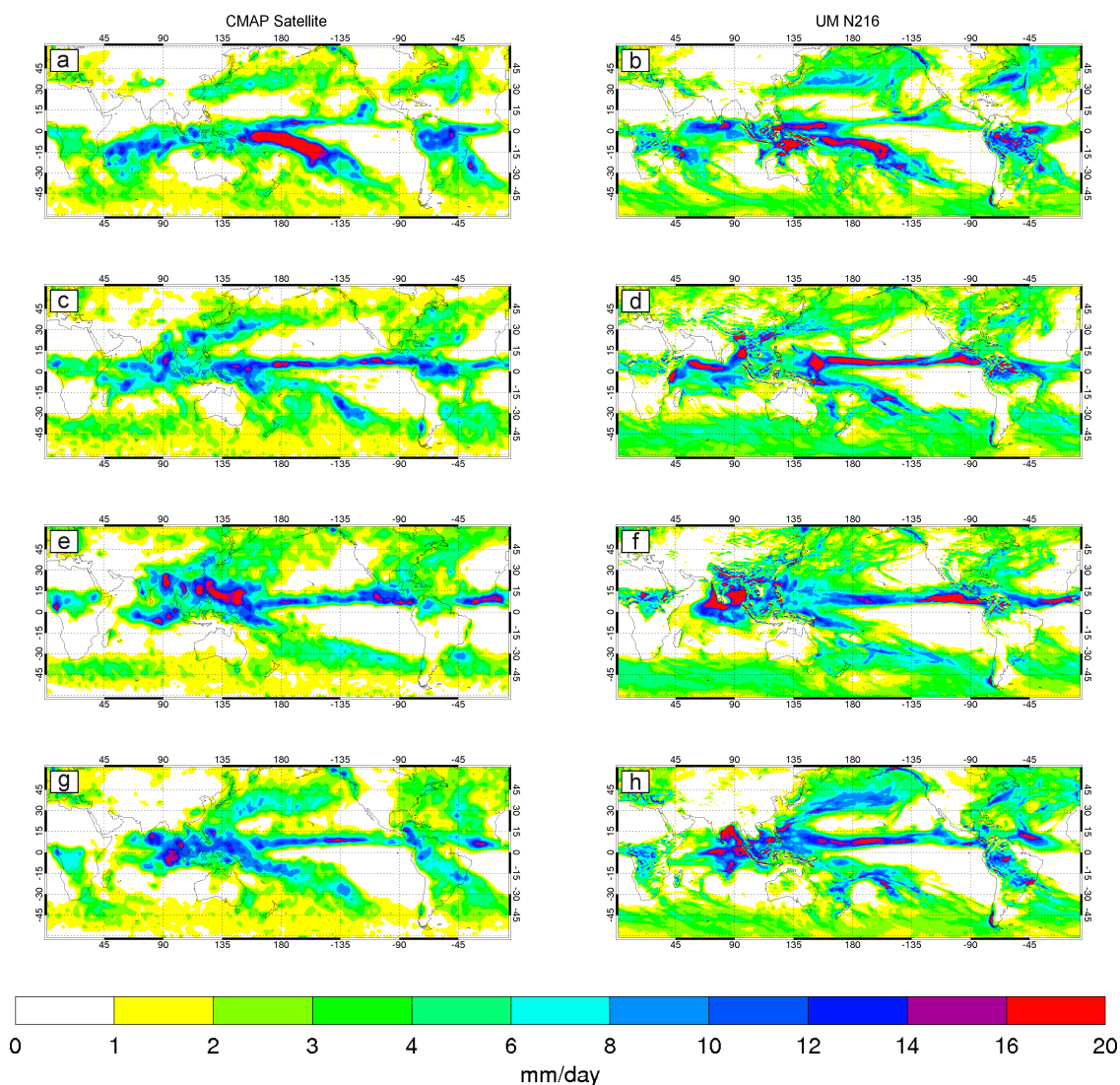


Fig. 4. Monthly mean CMAP precipitation rate satellite data (left column) and the UM forecast model experiment (right column) comparisons for February (a, b), May (c, d), August (e, f) and November (g, h) 2005.

and South America regions generally match the convective signatures and have high OLR correlations, as seen in Table 1. There are a few regions where, in comparison, the representation of the convective signatures is relatively poor. Over India in August, there is an over-estimation of precipitation rate and an under-estimation in OLR (i.e., high cloud) giving a greater CVRMSE of 10.85%. This suggests that the model is producing too much convection although the location is well represented with a spatial correlation coefficient of 0.83. As observed by Rossow and Pearl (2007) and Romps and Kuang (2009), large organised convective systems overshoot the level of neutral buoyancy more frequently than smaller ones. The amount of overshooting could be significantly larger in the model in August compared to observations which may have significance for dehydration and the

formation of cirrus cloud in the upper TTL and TST. Over the Maritime Continent and South America, where OLR is low due to deep convection, precipitation is generally over-estimated. However, this is not the case over Africa as the convective signature seen in OLR is not found in the corresponding precipitation rate. This illustrates that precipitation rate is not as useful an indicator as OLR for measuring the monthly mean distribution of deep tropical convection in the model.

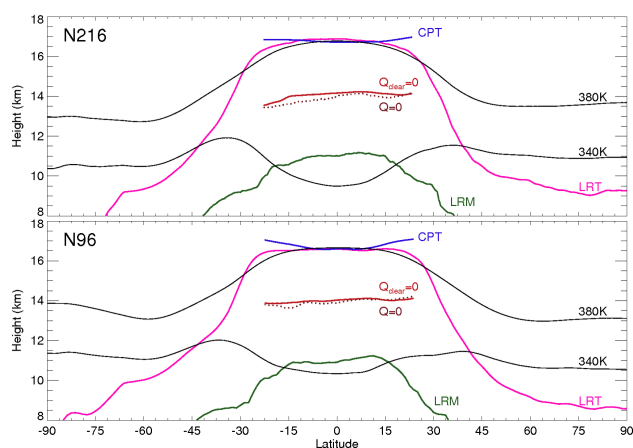


Fig. 5. Zonal and monthly mean TTL structures for November in the UM forecast (N216) and climate (N96) model setups. The lower TTL boundary is defined by the Lapse Rate Minimum (LRM, green line), and the tropical tropopause by the Cold Point Tropopause (CPT, blue line), the Lapse Rate Tropopause (LRT, pink line) and the 380K isentropic level (upper black line). The “clear-sky” ($Q_{\text{clear}} = 0$) and “all-sky” ($Q = 0$) levels of zero radiative heating are represented respectively by the solid and dotted red lines. The 340 K isentropic level (lower black line) is illustrated for reference regarding possible quasi-horizontal transport from the TTL into the extra-tropical lowermost stratosphere.

4 Tropical convection and the TTL

4.1 TTL structure

The TTL is the primary gateway from the troposphere into the stratosphere. Therefore, it is crucial that the TTL is well represented in global climate models if they are to capture the flux of water vapour and chemically active species (e.g., brominated compounds) through the tropical tropopause.

We have explored the longitudinal and seasonal variations of the modelled TTL. Preliminary timeseries studies for a single grid-point were investigated to understand how the TTL structure varies temporally (not shown). The LRM height is highly variable between 8–14 km in the tropics with a short response time to convection. We find that in convective regions the LRM is generally higher as described by Gettelman and Forster (2002). The levels of zero radiative heating ($Q_{\text{clear}} = 0$ and $Q = 0$) are not influenced much by convection but have a steady diurnal cycle with a range of ~ 1 km (here centred around ~ 14 – 14.5 km) as shortwave radiation changes.

In Fig. 5 we show the zonal and monthly mean TTL structure in our forecast (N216) model setup for November. We assess the height of the three commonly used tropical tropopause definitions; (1) the cold point tropopause (blue line), (2) the WMO lapse rate tropopause (pink line) and (3) a specified isentropic level, in this instance $\theta = 380$ K (upper black line).

The TTL base, the LRM, resides between 10–12 km between latitudes $\sim 20^\circ$ N– 20° S (green line). The $Q_{\text{clear}} = 0$ level (solid red line) and the $Q = 0$ level (dotted red line) separate the TTL vertically into an upper region of mean ascent and a lower region of mean subsidence.

As chemistry-climate models (CCMs) are used to assess the transport of tropospheric substances through the TTL we will also compare how horizontal resolution affects the structure of the TTL levels (see N96 in Fig. 5).

Generally, the zonal mean TTL structures in the two models mirror one another and are well defined. The LRM, $Q_{\text{clear}} = 0$ and $Q = 0$ levels all have well defined structures in the tropics between latitudes $\pm 20^\circ$. The $Q_{\text{clear}} = 0$ and $Q = 0$ levels surfaces are very close to each other at around 14 km. Above the LRM the air is clearly above the 340 K isentropic surface (lower black line) which connects the TTL and the extra-tropical lowermost stratosphere. Air lifted to this region can certainly be transported adiabatically (quasi-horizontal) into the stratosphere (e.g., Holton et al., 1995). Within the tropics the three tropical tropopause surfaces are all close to each other and confined to below 17 km. Within mid-latitudes ($\sim \pm 30$ – 50°), the CPT diverges under the influence of the subtropical jets and becomes more isothermal. This is the region of the tropopause break and so becomes unrepresentative of the tropopause (for this reason the CPT surface is not shown for latitudes greater than 30°).

The UM is seen here to capture the same TTL structure at two different resolutions. There is thus a similar level of mean detrainment from the large-scale Hadley circulation and deep convection (LRM), a similar forcing by stratospheric ozone and pumping by the Brewer-Dobson circulation (CPT and LRT) and a similar radiative balance by absorption and emission of H_2O , O_3 and CO_2 ($Q = 0$ and $Q_{\text{clear}} = 0$).

As the LRM, $Q_{\text{clear}} = 0$, $Q = 0$ and CPT levels are only well defined within the tropics, the study of convectively driven transport to the TTL, followed by radiatively driven ascent or subsidence (next), will only be made between latitudes $\pm 20^\circ$. This is, in any case, the region where deep convection is likely to be most important on average.

4.2 CPT Temperature

Water vapour is important for both the radiative and chemical budget of the stratosphere. It is therefore important that models correctly represent the CPT (height and temperature) and the coupling with convection in order to model deep convectively driven injections of water vapour and tropospheric material through the TTL and into the stratosphere. In Fig. 6, we show the temperature of the monthly mean CPT for the four monthly experiments. The tropical tropopause temperature is higher between May and October and lower between November and April in agreement with MLS satellite observations (Schwartz et al., 2008). Consequently, the water vapour mixing ratios entering the stratosphere also exhibits

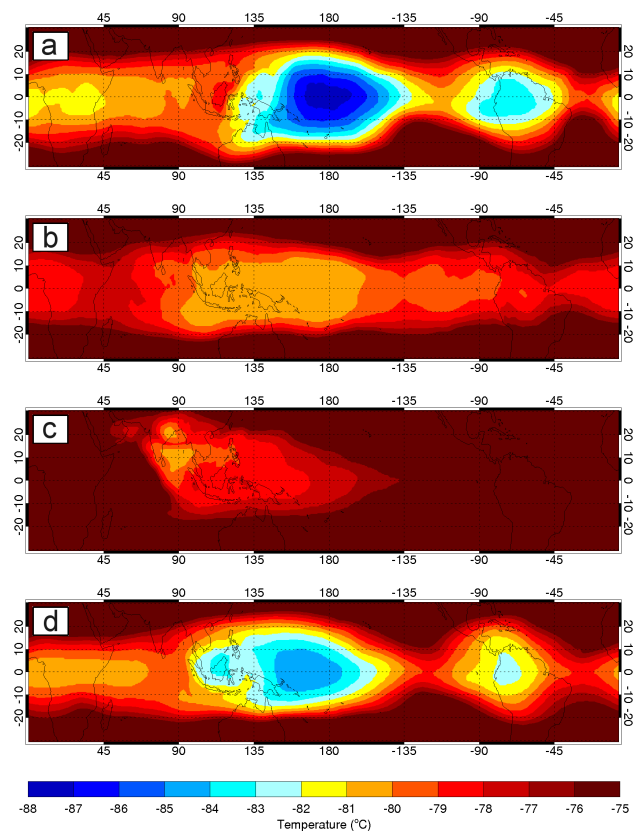


Fig. 6. Monthly mean temperature distribution at the cold point tropopause (CPT, around ~ 17 km and 100 hPa) in the UM global forecast model. February (a), May (b), August (c) and November (d).

an annual cycle (moist and dry, respectively), i.e., the stratospheric tape recorder (Mote et al., 1996).

In all four monthly integrations, the Maritime Continent and West-Central Pacific regions show a marked cold region within $90\text{--}135^\circ\text{E}$ and $20^\circ\text{N}\text{--}20^\circ\text{S}$ (Fig. 6). The Northern Hemisphere winter months show a more pronounced cold tropopause (-88°C to -84°C) in these regions which is comparable with the seasonal cycle as proposed by Newell and Gould-Stewart (1981) and Mote et al. (1996). May and August are relatively warmer (-81°C to -75°C) over all regions in comparison. These seasonal variations agree with the stratospheric tape recorder (Mote et al., 1996).

4.3 Vertical convective transport

In this section we analyse the vertical extent of tropical convection, with respect to the TTL structure, taking meridional averages between latitudes $\pm 20^\circ$ in the model integrations. This analysis highlights where deep convection occurs; the vertical extent of convection; where material can detrain from and influence the structure of the TTL. All of these are important for tropospheric-stratospheric transport.

The vertical extent of tropical convection is shown in Fig. 7 for the four months. Our diagnostic, convective cloud top PDF, is shown by the Panels on the left and is calculated from the convective cloud top height field as described in Sect. 2. The second diagnostic (right) is simply the monthly mean convective mass flux averaged between latitudes $\pm 20^\circ$.

The convective cloud top PDFs highlight the level of mean convective outflow showing a clear distinction between shallow oceanic convection reaching 2–6 km and deeper continental convection which frequently reaches the lower TTL. This is less clear in the convective mass flux diagnostic. As shown by both convective diagnostics, equatorial Africa, the Maritime Continent, West Pacific and South America regions all show that convection could potentially lift surface emitted species from the lower troposphere and detrain them within the TTL. As shown by the convective cloud top PDF there is a clear marked level of convective outflow (~ 13 km), above which the number of convective cloud tops decreases steadily with height. This is consistent with the findings of Folkins et al. (1999), Gettelman et al. (2002) and Gettelman and Forster (2002). Above the convective clouds, air becomes increasingly influenced by the relatively slow radiative transport, as opposed to rapid convective mixing. Hence, the residence time of air increases in this region (Fueglistaler et al., 2004). Consequently, air that reaches the lower TTL has a greater chance of being transported to the extra-tropical lowermost stratosphere across isentropic surfaces of potential temperatures greater than 340 K (see Fig. 5).

Generally, in the model, convection is deeper and more frequent over the Maritime Continent, West Pacific, and also over the Indian Ocean during the monsoon in August. This is illustrated by the convective cloud top PDF where, for all months, up to 25% of the grid-points between latitudes $\pm 20^\circ$ show convection reaching the lower TTL between 12–14 km. The convective mass flux shows similarly that deep convective “pillars” lift air rapidly from around 4–5 km up to 12–14 km (see e.g., November at 90°E). This suggests that the time it takes for surface air to reach 4–5 km is important for setting the mixing ratio of VSLS that will enter the base of the “convective elevator” and thus define the TTL entry concentrations.

During the February and November integrations over the West Pacific ($100\text{--}160^\circ\text{E}$), there are modelled mass fluxes of up to $20\text{ kg/m}^2/\text{hr}$ that reach well into the upper TTL. The location (see Fig. 6) seems to coincide closely with the tropopause cold region allowing for the possibility of direct injection of air and subsequent freeze-drying (e.g., Sherwood and Dessler, 2000). However, by analysing a timeseries of a single convective grid-point (not shown), we found that the water vapour mixing ratios in the TTL actually showed an increase after deep convective events (> 14 km). This is consistent with evidence which suggests that convection on average actually hydrates the TTL (Corti et al., 2008).

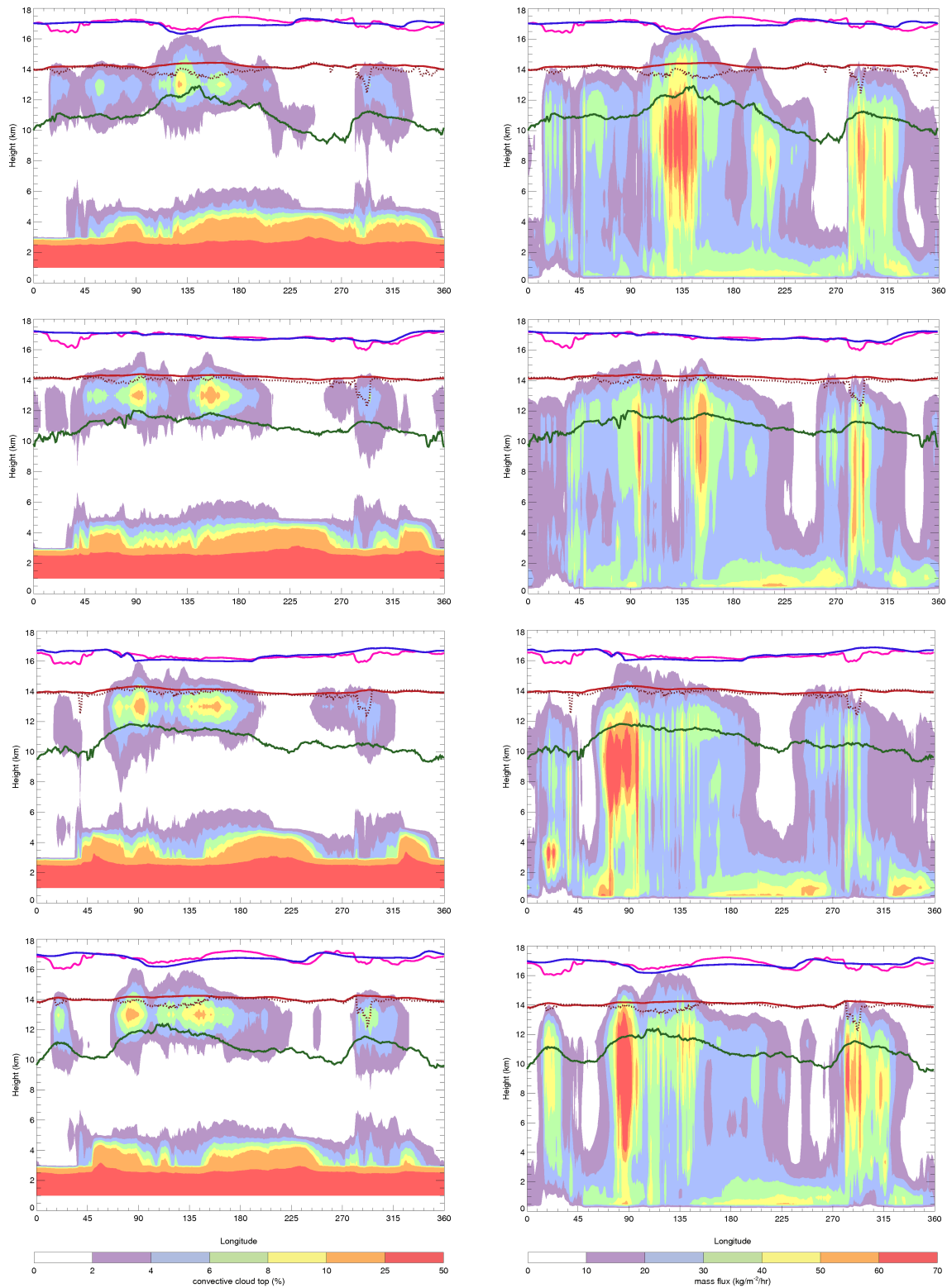


Fig. 7. Assessing the longitudinal-vertical distribution of tropical convection between latitudes 20°N – 20°S using the “convective cloud top PDFs” (left column) and monthly mean convective mass fluxes (right column) for the 4 modelled integrations; February, May, August and November (rows top to bottom, respectively). The TTL levels are represented by the coloured lines as shown by the legend in Fig. 2.

However, as the model's convective transport is almost entirely parameterised (with no microphysics) and the resolution is too coarse to represent the complex microphysics, it relies on the parametrisation schemes for water vapour cycling.

Therefore, a cloud-resolving tropical wide simulations maybe a good way to further investigate the impact of tropical convection on the transport of water vapour and VLSLs.

For the most part, the two convective diagnostics show the same regional and seasonal variations of convective activity although there are some differences. In November, there is a significantly deep convective “pillar” at 90° E over the Maritime Continent extending from 4–14 km which dwarfs other convective features seen in other regions (Fig. 7 lower right panel); however, the location and magnitude are not highlighted in the convective cloud top PDF. Also, the convective mass fluxes in May seem to be relatively smaller than for the other months over all regions with low values above the $Q_{\text{clear}} = 0$ level. However, the convective cloud top PDF for May does not look very different from the other months. Clearly, the two convective diagnostics can sometimes give different pictures of convective activity (at least for these months) as also shown in Fig. 1.

The height of the LRM (green line) is highly correlated with convective activity. This can be seen for all the integrations where in convective regions the height increases up to ~ 13 km (as seen in February), and decreases as low as 9 km in non-convective regions (e.g., East Pacific). The $Q_{\text{clear}} = 0$ (red line) and $Q = 0$ (dotted red line) levels overlap at most latitudes although over regions of active convection an anti-correlation is evident in the $Q = 0$ level due to increased cloud cover scattering shortwave radiation. The monthly mean $Q_{\text{clear}} = 0$ level is mostly uniform at around 14 km throughout the tropics and has no obvious seasonal cycle which is consistent with Gettelman and Forster (2002). The height of the meridional mean $Q_{\text{clear}} = 0$ level in the UM is lower than the range (~ 15 – 15.5 km) calculated by Folkins et al. (1999), Gettelman and Forster (2002) and Gettelman et al. (2004) which highlights the current level of uncertainty in the TTL's radiative balance.

The height of the CPT (blue line) and the LRT (pink line) are very similar at most longitudes although over regions of high orography (e.g., the Andes) the LRT height decreases by around 1 km. The CPT and LRT heights are lower in August dropping to less than 16 km in many areas between 90–180° E, although convection is not significantly different compared with the other months. The large-scale CPT and LRT height is not dominated (at least directly) by convective activity in agreement with the analysis of Gettelman and Forster (2002) and is likely driven by the strength of the Brewer-Dobson circulation (Yulaeva et al., 1994). This is evident in February where the large-scale CPT is higher (in the absence of deep convection) over the West and Central Pacific. However, over regions where large convective mass fluxes are evident up to 16 km (as seen in February and

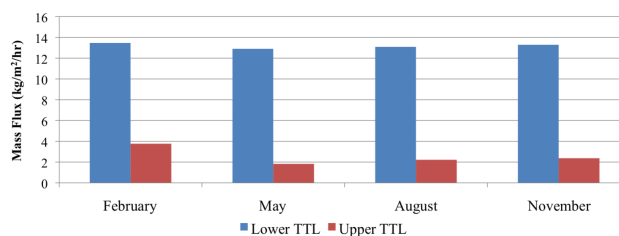


Fig. 8. Monthly mean convective mass fluxes integrated over all longitudes between latitudes 20° N–20° S for the upper (red bars) and lower (blue bar) TTL where the TTL boundaries are defined by the monthly mean LRM, $Q_{\text{clear}} = 0$ and CPT levels.

November in Fig. 7), the local CPT height is slightly lower than average. This may be explained by several factors: adiabatic cooling above convection, an indirect dynamic response to the release of latent heat at lower levels (Highwood and Hoskins, 1998), radiative cooling associated with thick convective clouds (Gage et al., 1991; Norton, 2001) or by upwelling of ozone poor air reducing radiative heating. A colder tropopause may also increase convective instability triggering further convection although this is hard to prove by measurements. Consequently, in the ‘model world’ at least, deep convection and tropopause temperatures are coupled; although the details are still uncertain.

Figure 7 gives some insight into how tropical convective mass fluxes vary with season. In Fig. 8 we quantify how the convective transport changes month-by-month at a more global-scale by assessing the tropical ($\pm 20^\circ$) monthly mean mass flux in the lower TTL (blue bars) and the upper TTL (red bars). It is clear that all four months are very similar in the lower TTL (~ 13 kg/m²/hr) suggesting that the amount of tropospheric trace species entering the TTL, and reaching the $Q_{\text{clear}} = 0$ level, is broadly the same all year round; i.e., no seasonal cycle. This will only be true, of course, if the trace species’ source has a small annual cycle in emissions and spatial variation. However, in February the upper TTL exhibits around twice the convective mass flux compared to the other months. Again, this coincides with the very low tropopause temperatures over the Maritime Continent and West Pacific suggesting that CPT temperature may be significant for allowing convection to penetrate deep in to the TTL and up to the tropopause as suggested by Gettelman et al. (2002). This may therefore be a region and time period for potential preferential TST of VLSL emission, especially over the Maritime Continent which is a potentially important source of $CHBr_3$ (e.g., Yokouchi et al., 2005) and other brominated and iodinated biogenic short-lived compounds.

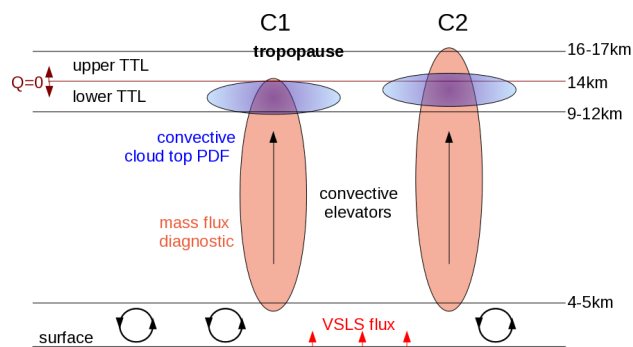


Fig. 9. A simplified sketch of modelled vertical structures of tropical convection, as represented by cloud top height PDFs (blue ovals) and convective mass fluxes (orange ovals) relative to TTL levels. For C1 type convection, both convective diagnostics generally reach around or below the $Q = 0$ level. For C2 type convection, while the cloud top height PDF maximum reaches slightly above the $Q = 0$ zero level, convective mass fluxes penetrate well into the upper TTL.

5 Conclusions

We conducted case studies with the Unified Model based on a weather forecast setup (N216, $\sim 0.83^\circ \times \sim 0.56^\circ$, ~ 60 km). Four monthly integrations from the year 2005 have been performed starting the model from UK Met Office assimilated data. The structure and behaviour of modelled tropical convection was analysed, with a focus on assessing how convection penetrates into, and through, the TTL. Our primary interest lies in assessing the suitability of the model for transporting ozone-depleting VLSL into the stratosphere.

To evaluate the model we used monthly mean OLR as an indicator of the spatial distribution of deep tropical convection (Fig. 1).

Even though convection is parameterised in the model, recent studies find that this very model setup is suitable for transporting VLSL as shown by comparing the distribution of modelled high cloud to observations (Russo et al., 2010) and vertical transport of idealised short-lived tracers (Hoyle et al., 2010).

The modelled OLR correlates well with NOAA satellite observations, suggesting that the location of tropical convection was well represented in the model. Although some observations have suggested that convective clouds might regularly reach up to 18–20 km (Sassen et al., 2008; Nazaryan et al., 2008), such events are not represented in our model as the horizontal resolution is not high enough to resolve clouds or their overshooting turrets. However a recent observational study by Aumann and DeSouza-Machado (2010) suggests that such events may be wrongly detected. To improve the representation of deep tropical convection a global, or tropical wide, cloud-resolving model could be adopted although this would require significantly more computational power and data storage.

The modelled vertical structures of convection are sketched in Fig. 9 represented by cloud top height PDFs (blue ovals) and convective mass fluxes (orange ovals). In our model, we are able to distinguish between two configurations, here labelled C1 and C2. In both cases air is lofted rapidly from around 4–5 km. Therefore, the time it takes for surface air to reach this altitude is important for setting the mixing ratio of VLSL that will enter the base of the “convective elevator” and thus define the TTL entry concentrations. For the C1 type, the convective mass fluxes stop around the $Q = 0$ level, and the maximum of the cloud top height PDF is solely in the lower TTL. Convective injections into the lower TTL may be followed by quasi-horizontal transport into the extra-tropical lowermost stratosphere (Levine et al., 2007). For C2 type, convective mass fluxes penetrate the upper TTL, and the maximum of the cloud top height PDF is higher compared to C1, reaching slightly above the $Q = 0$ zero level. Air that reaches this region can undergo slow radiatively-driven ascent into the tropical lower stratosphere.

Many studies use satellite data to derive cloud properties which are similar to the modelled cloud top height PDFs and this information is utilised as a proxy for vertical transport into the tropical lower stratosphere (e.g., Liu and Zipser, 2005). In the C2 configuration, although mass fluxes penetrate into the upper TTL, the convective cloud top PDF indicates only a small convective impact on this region. Therefore remote sensing studies can not clearly distinguish between C1 and C2 events and, as a consequence, quantitative estimates of transport might be biased.

For our model integrations, the monthly mean convective diagnostics show most commonly the C1 type. This clear confinement of convection to heights below 14 km is in good agreement with Folkins et al. (2000). In February, over the Maritime Continent, our model produces clear evidence for C2 events (see Fig. 7). In the other months analysed (May, August and November), the monthly mean cloud top PDFs and convective mass fluxes indicate that C2 type events are less pronounced. In our model, the preferential location of C2 events for all months is around the Maritime Continent region, showing a clear seasonality.

The mean tropopause height is lower over regions where cloud top PDFs reach above the $Q = 0$ level. In such cases, the lower tropopause height, in conjunction with mass fluxes reaching the upper TTL, is likely to increase the potential for troposphere-stratosphere transport, as suggested by the analysis of the February integration (Fig. 7). With high emissions of VLSL in coastal regions of the Maritime Continent, rapid uplift from the surface to 4–5 km (e.g., sea breeze convergence), and subsequent fast transport by C2 events, the model indicates a potential for injecting ozone-depleting species into the tropical lower stratosphere. This mechanism could contribute to the elevated levels of observed stratospheric bromine, which is not accounted for by many chemistry-climate models (WMO, 2006).

Acknowledgements. We acknowledge Dr Jackson from UKMO for providing the data assimilated initial conditions and Dr Chemel from the University of Hertfordshire for assistance and useful discussions. Interpolated OLR and CMAP data are provided by the NOAA/OAR/ESRL PSD, Boulder, Colorado, USA, from their website (<http://www.cdc.noaa.gov/>).

Edited by: M. Dameris

References

- Aumann, H. H. and DeSouza-Machado, S. G.: Deep convective clouds at the tropopause, *Atmos. Chem. Phys. Discuss.*, 10, 16475–16496, doi:10.5194/acpd-10-16475-2010, 2010.
- Brewer, A.: Evidence for a world circulation provided by the measurements of helium and water vapour distribution in the Stratosphere, *Q. J. Roy. Meteorol. Soc.*, 75, 351–63, 1949.
- Corti, T., Luo, B. P., de Reus, M., Brunner, D., Cairo, F., Mahoney, M. J., Martucci, G., Matthey, R., Mitev, V., dos Santos, F. H., Schiller, C., Shur, G., Sitnikov, N. M., Spelten, N., Vössing, H. J., Borrmann, S., and Peter, T.: Unprecedented evidence for deep convection hydrating the tropical stratosphere, *Geophys. Res. Lett.*, 35, L10810, doi:10.1029/2008GL033641, 2008.
- Danielsen, E. F.: In situ evidence of rapid, vertical, irreversible transport of lower tropospheric air into the lower tropical stratosphere by convective cloud turrets and by larger-scale upwelling in tropical cyclones, *J. Geophys. Res.-Atmos.*, 98, 8665–8681, 1993.
- Davies, T., Cullen, M., Malcolm, A., Mawson, M., Staniforth, A., White, A., and Wood, N.: A new dynamical core for the Met Office's global and regional modelling of the atmosphere, *Q. J. Roy. Meteorol. Soc.*, 131, 1759–1782, doi:10.1256/qj.04.101, 2005.
- Edwards, J. and Slingo, A.: Studies with a flexible new radiation code. I: Choosing a configuration for a large-scale model, *Q. J. Roy. Meteorol. Soc.*, 122, 689–719, 1996.
- Essery, R. L. H., Best, M. J., Betts, R. A., Cox, P. M., and Taylor, C. M.: Explicit representation of subgrid heterogeneity in a GCM land surface scheme, *J. Hydrometeorol.*, 4, 530–543, 2003.
- Folkens, I., Loewenstein, M., Podolske, J., Oltmans, S., and Proffitt, M.: A barrier to vertical mixing at 14 km in the tropics: Evidence from ozonesondes and aircraft measurements, *J. Geophys. Res.-Atmos.*, 104, 22095–22102, 1999.
- Folkens, I., Oltmans, S., and Thompson, A.: Tropical convective outflow and near surface equivalent potential temperatures, *Geophys. Res. Lett.*, 27, 2549–2552, 2000.
- Fritsch, J. and Chappell, C.: Numerical prediction of convectively driven mesoscale pressure systems. I: Convective parameterization, *J. Atmos. Sci.*, 37, 1722–1733, 1980a.
- Fritsch, J. and Chappell, C.: Numerical prediction of convectively driven mesoscale pressure systems. II: Mesoscale model, *J. Atmos. Sci.*, 37, 1734–1762, 1980b.
- Fueglistaler, S., Wernli, H., and Peter, T.: Tropical troposphere-to-stratosphere transport inferred from trajectory calculations, *J. Geophys. Res.-Atmos.*, 109, D03108, doi:10.1029/2003JD004069, 2004.
- Fueglistaler, S., Dessler, A. E., Dunkerton, T. J., Folkens, I., Fu, Q., and Mote, P. W.: Tropical tropopause layer, *Rev. Geophys.*, 47, RG1004, doi:10.1029/2008RG000267, 2009.
- Gage, K. S., Mcafee, J. R., Carter, D. A., Ecklund, W. L., Riddle, A. C., Reid, G. C., and Balsley, B. B.: Long-term mean vertical motion over the tropical Pacific – wind-profiling Doppler radar measurements, *Science*, 254, 1771–1773, 1991.
- Gettelman, A. and Forster, P. M.: A climatology of the tropical tropopause layer, *J. Meteor. Res. Jpn.*, 80, 911–924, 2002.
- Gettelman, A., Salby, M., and Sassi, F.: Distribution and influence of convection in the tropical tropopause region, *J. Geophys. Res.-Atmos.*, 107(D10), 4080, doi:10.1029/2001JD001048, 2002.
- Gettelman, A., Forster, P., Fujiwara, M., Fu, Q., Vomel, H., Gohar, L., Johanson, C., and Ammerman, M.: Radiation balance of the tropical tropopause layer, *J. Geophys. Res.-Atmos.*, 109, D07103, doi:10.1029/2003JD004190, 2004.
- Grant, A.: Cloud-base fluxes in the cumulus-capped boundary layer, *Q. J. Roy. Meteorol. Soc.*, 127, 407–421, 2001.
- Grant, A. L. M. and Brown, A. R.: A similarity hypothesis for shallow-cumulus transports, *Q. J. Roy. Meteorol. Soc.*, 125, 1913–1936, 1999.
- Gregory, D. and Rowntree, P.: A mass flux convection scheme with representation of cloud ensemble characteristics and stability-dependent closure, *Mon. Weather Rev.*, 118, 1483–1506, 1990.
- Highwood, E. J. and Hoskins, B. J.: The tropical tropopause, *Q. J. Roy. Meteorol. Soc.*, 124, 1579–1604, 1998.
- Holton, J. and Gettelman, A.: Horizontal transport and the dehydration of the stratosphere, *Geophys. Res. Lett.*, 28, 2799–2802, 2001.
- Holton, J. R., Haynes, P. H., McIntyre, M. E., Douglass, A. R., Rood, R. B., and Pfister, L.: Stratosphere-troposphere exchange, *Rev. Geophys.*, 33, 403–439, 1995.
- Hoyle, C. R., Marécal, V., Russo, M. R., Arteta, J., Chemel, C., Chipperfield, M. P., D'Amato, F., Dessens, O., Feng, W., Harris, N. R. P., Hosking, J. S., Morgenstern, O., Peter, T., Pyle, J. A., Reddman, T., Richards, N. A. D., Telford, P. J., Tian, W., Viciani, S., Wild, O., Yang, X., and Zeng, G.: Tropical deep convection and its impact on composition in global and mesoscale models – Part 2: Tracer transport, *Atmos. Chem. Phys. Discuss.*, 10, 20355–20404, doi:10.5194/acpd-10-20355-2010, 2010.
- Levine, J. G., Braesicke, P., Harris, N. R. P., Savage, N. H., and Pyle, J. A.: Pathways and timescales for troposphere-to-stratosphere transport via the tropical tropopause layer and their relevance for very short lived substances, *J. Geophys. Res.-Atmos.*, 112, D04308, doi:10.1029/2005JD006940, 2007.
- Li, D. and Shine, P.: A 4-Dimensional Ozone Climatology for UGAMP Models, UGAMP Internal Report, 1995.
- Liebmann, B. and Smith, C. A.: Description of a complete (interpolated) outgoing longwave radiation dataset, *B. Am. Meteorol. Soc.*, 77, 1275–1277, 1996.
- Liu, C. T. and Zipser, E. J.: Global distribution of convection penetrating the tropical tropopause, *J. Geophys. Res.-Atmos.*, 110, D23104, doi:10.1029/2005JD006063, 2005.
- Lock, A. P., Brown, A. R., Bush, M. R., Martin, G. M., and Smith, R. N. B.: A new boundary layer mixing scheme. Part I: Scheme description and single-column model tests, *Mon. Weather Rev.*, 128, 3187–3199, 2000.
- Martin, G. M., Ringer, M. A., Pope, V. D., Jones, A., Dearden, C., and Hinton, T. J.: The physical properties of the atmosphere in the new Hadley Centre Global Environmental Model (HadGEM1). Part I: Model description and global climatology, *J. Climate*, 19, 1274–1301, 2006.

- Mote, P., Rosenlof, K., McIntyre, M., Carr, E., Gille, J., Holton, J., Kinnersley, J., Pumphrey, H., Russell, J., and Waters, J.: An atmospheric tape recorder: The imprint of tropical tropopause temperatures on stratospheric water vapor, *J. Geophys. Res.-Atmos.*, 101, 3989–4006, 1996.
- Nazaryan, H., McCormick, M. P., and Menzel, W. P.: Global characterization of cirrus clouds using CALIPSO data, *J. Geophys. Res.-Atmos.*, 113, D16211, doi:10.1029/2007JD009481, 2008.
- Newell, R. and Gould-Stewart, S.: A Stratospheric Fountain, *J. Atmos. Sci.*, 38, 2789–2796, 1981.
- Norton, W. A.: Longwave Heating of the Tropical Lower Stratosphere, *Geophys. Res. Lett.*, 28(19), 3653–3656, doi:10.1029/2001GL013379, 2001.
- Parker, D., Jackson, M., and Horton, E. B.: The 1961–1990 GISST2.2 Sea Surface Temperature and Sea Ice Climatology, The Hadley Centre Climate Research Technical Note No. 63, 1995.
- Petch, J. C., Willett, M., Wong, R. Y., and Woolnough, S. J.: Modelling suppressed and active convection. Comparing a numerical weather prediction, cloud-resolving and single-column model, *Q. J. Roy. Meteorol. Soc.*, 133, 1087–1100, doi:10.1002/qj.109, 2007.
- Ricaud, P., Barret, B., Attie, J. L., Motte, E., Le Flochmoen, E., Teyssedre, H., Peuch, V. H., Livesey, N., Lambert, A., and Pommereau, J. P.: Impact of land convection on troposphere-stratosphere exchange in the tropics, *Atmos. Chem. Phys.*, 7, 5639–5657, doi:10.5194/acpd-7-5639-2007, 2007.
- Romps, D. M. and Kuang, Z.: Overshooting convection in tropical cyclones, *Geophys. Res. Lett.*, 36, L09804, doi:10.1029/2009GL037396, 2009.
- Rossov, W. B. and Pearl, C.: 22-Year survey of tropical convection penetrating into the lower stratosphere, *Geophys. Res. Lett.*, 34, L04803, doi:10.1029/2006GL028635, 2007.
- Russo, M. R., Marécal, V., Hoyle, C. R., Arteta, J., Chemel, C., Chipperfield, M. P., Dessens, O., Feng, W., Hosking, J. S., Telford, P. J., Wild, O., Yang, X., and Pyle, J. A.: Tropical deep convection and its impact on composition in global and mesoscale models - Part I: Meteorology and comparison with observations., *Atmos. Chem. Phys. Discuss.*, 10, 19469–19514, doi:10.5194/acpd-10-19469-2010, 2010.
- Salawitch, R., Weisenstein, D., Kovalenko, L., Sioris, C., Wennberg, P., Chance, K., Ko, M., and McLinden, C.: Sensitivity of ozone to bromine in the lower stratosphere, *Geophys. Res. Lett.*, 32, L05811, doi:10.1029/2004GL021504, 2005.
- Sassen, K., Wang, Z., and Liu, D.: Global distribution of cirrus clouds from CloudSat/CloudAerosol Lidar and Infrared Pathfinder Satellite Observations (CALIPSO) measurements, *J. Geophys. Res.-Atmos.*, 113, D00A12, doi:10.1029/2008JD009972, 2008.
- Schwartz, M. J., Lambert, A., Manney, G. L., Read, W. G., Livesey, N. J., Froidevaux, L., Ao, C. O., Bernath, P. F., Boone, C. D., Cofield, R. E., Daffer, W. H., Drouin, B. J., Fetzer, E. J., Fuller, R. A., Jarnot, R. F., Jiang, J. H., Jiang, Y. B., Knosp, B. W., Krueger, K., Li, J. L. F., Mlynczak, M. G., Pawson, S., Russell, J. M., I., Santee, M. L., Snyder, W. V., Stek, P. C., Thurstans, R. P., Tompkins, A. M., Wagner, P. A., Walker, K. A., Waters, J. W., and Wu, D. L.: Validation of the Aura Microwave Limb Sounder temperature and geopotential height measurements, *J. Geophys. Res.-Atmos.*, 113, D15S11, doi:10.1029/2007JD008783, 2008.
- Seidel, D., Ross, R., Angell, J., and Reid, G.: Climatological characteristics of the tropical tropopause as revealed by radiosondes, *J. Geophys. Res.-Atmos.*, 106, 7857–7878, 2001.
- Sherwood, S. C. and Dessler, A. E.: On the control of stratospheric humidity, *Geophys. Res. Lett.*, 27, 2513–2516, 2000.
- Sherwood, S. C. and Dessler, A. E.: A model for transport across the tropical tropopause, *J. Atmos. Sci.*, 58, 765–779, 2001.
- Sinnhuber, B. M. and Folkins, I.: Estimating the contribution of bromoform to stratospheric bromine and its relation to dehydration in the tropical tropopause layer, *Atmos. Chem. Phys.*, 6, 4755–4761, doi:10.5194/acp-6-4755-2006, 2006.
- Thuburn, J. and Craig, G.: On the temperature structure of the tropical stratosphere, *J. Geophys. Res.-Atmos.*, 107(D2), 4017, doi:10.1029/2001JD000448, 2002.
- Wilson, D. R. and Ballard, S. P.: A microphysically based precipitation scheme for the UK Meteorological Office Unified Model, *Q. J. Roy. Meteorol. Soc.*, 125, 1607–1636, 1999.
- WMO: (World Meteorological Organization), Scientific Assessment of Ozone Depletion: 2006, Global Ozone Research and Monitoring Project – Report No. 50, Geneva, Switzerland, 572 pp., 2007.
- Xie, P. and Arkin, P.: Global precipitation: A 17-year monthly analysis based on gauge observations, satellite estimates, and numerical model outputs, *Bull. Am. Meteorol. Soc.*, 78, 2539–2558, 1997.
- Yokouchi, Y., Hasebe, F., Fujiwara, M., Takashima, H., Shiotani, M., Nishi, N., Kanaya, Y., Hashimoto, S., Fraser, P., Toom-Saunty, D., Mukai, H., and Nojiri, Y.: Correlations and emission ratios among bromoform, dibromochloromethane, and dibromomethane in the atmosphere, *J. Geophys. Res.*, 110, doi:10.1029/2005JD006303, 2005.
- Yulaeva, E., Holton, J. R., and Wallace, J. M.: On the cause of the annual cycle in tropical lower-stratospheric temperatures, *J. Atmos. Sci.*, 51, 169–174, 1994.